Extended X-Ray Absorption Fine Structure Studies on Local Structure in Amorphous $LaNi_{5.0}$ Films

Tomoyoshi SUENOBU, Hiroki SAKAGUCHI, Takaharu TSUJI, Hiroyoshi KANAI,† Satohiro YOSHIDA,†† and Gin-ya ADACHI*

Department of Applied Chemistry, Faculty of Engineering, Osaka University, Yamadaoka, Suita, Osaka 565
†Faculty of Living Science, Kyoto Prefectural University, Shimogamo, Sakyoku, Kyoto 606
††Department of Hydrocarbon Chemistry and Division of Molecular Engineering, Kyoto University, Kyoto 606

(Received July 15, 1991)

Analyses of the local structure around La and Ni atoms in amorphous $LaNi_{5.0}$ films have been performed using the extended X-ray absorption fine structure (EXAFS), and the effect of the structure on the difference of hydrogen absorption characteristics between the amorphous and crystalline $LaNi_{5.0}$ has been elucidated. The lengthening of interatomic distances for the Ni–Ni and La–Ni pairs, respectively, was observed for the amorphous samples in comparison with the crystalline ones. A part of the hydrogen sites existed in the crystalline $LaNi_5$ was distorted in the amorphous one. Since the hydrogen atoms appear to be difficult to enter these sites distorted, the hydrogen content in the amorphous $LaNi_5$ is smaller than that in the crystalline one.

Amorphous $LaNi_5$ films have attracted considerable technological and scientific interest, such as hydrogen purification, catalysis, and batteries[1–3] Their physical and chemical properties have been found to be much different from those of the crystalline sample.[4–7] The amorphous $LaNi_5$ film has been known not to pulverize after repeated hydrogenation–dehydrogenation cycling, and absorbs hydrogen less than a half of the amount taken up by the crystalline bulk.[5,7] These differences of properties appear to be closely related to the structure of the films, so that it is necessary to obtain the detailed structural information at an atomic level.

In the present study, the local structure around La and Ni atoms in the amorphous $LaNi_{5.0}$ films is clarified by means of EXAFS, and the results are compared with those in the crystalline sample. The relationship between the structure and the hydrogen absorption characteristics is discussed.

Experimental

The $LaNi_{5.0}$ amorphous films (ca. 1 μm thick which was determined by direct observation of the cross section of the sample using a scanning electron microscope.) were deposited on a polyimide membrane (Kapton, 40 μm thick, Toray-du Pont Co., Ltd.) at room temperature by using sputtering method.[4,6,7] For the sputtering, parameters of 0.395-Pa Argon pressure (99.999%) and a radio-frequency generating power of 400 W were employed for all sputtered samples. The sputtering target consisted of a disk in which 98% of the surface area is $LaNi_{4.8}$ (33.0 wt% La, 66.8 wt% Ni) and 2% is $LaNi_{3.0}$. The La–Ni alloys were supplied by Santoku Metal Industry, Kobe, Japan. X-Ray diffraction measurements were made to verify the amorphous state. Their homogeneity and stoichiometry were checked by means of X-ray fluorescent spectroscopy and X-ray photoelectron spectroscopy. The films precisely having a composition of $LaNi_{5.0}$ were used for the EXAFS measurements. The $LaNi_{5.0}$ crystalline powder and commercially available Ni foil (5 μm thick, 99.98% pure, The Japan Lamp Industries) were used as reference materials. The crystalline $LaNi_{5.0}$ alloy film with a crystallinity of 80% was prepared on a stainless-steel substrate at 530 K by sputtering. The film was peeled from the substrate with an adhesive tape, and the resulting film was applied to the EXAFS measurements. The crystallinity of the film was determined from the heat of crystallization which was estimated by the differential scanning calorimetry (DSC).[7]

The measurement of X-ray absorption spectra (XAS) were performed by means of synchrotron radiation employing the EXAFS facilities of BL-7C of the Photon Factory in the National Laboratory for High-Energy Physics, Tsukuba, Japan. An Si(111) double crystal monochromator was used to monochromatize the X-rays from a 2.5-GeV positron storage ring. The ring current was between 350.5 and 246.9 mA. EXAFS spectra were collected at the Ni K- and La L_{III}-edges. The focusing mirror was used to reduce higher harmonics at the La edge. Energy resolution of 1.4 eV can be achieved at the Ni K-edge (8331.7 eV) when a source-size is not considered. The total thickness of the $LaNi_{5.0}$ films used for the X-ray absorption measurements were about 35 and 20 μm for the La and Ni edges respectively. All the XAS data were obtained at 220 K. Analyses of the EXAFS data were performed with a "KABO" program in the FACOM M382 computer system at the Data Processing Center, Kyoto University, Japan.

The photon energy was calibrated by the characteristic inflection point at the edge of the absorption spectrum of the standard Ni foil (5 μm thick, 8331.7 eV). The EXAFS oscillatory part $\chi(E)$ above the absorption edge was extracted from the XAS data using a simple equation of $A/E^{2.75}$ instead of Victoreen formula and normalized as described elsewhere.[8–10] The photoelectron wave vector k is related to the photon energy E expressed by $k=2\pi[2m(E-E_0)]^{1/2}/h$, where m is mass of an electron, h, Planck's constant, E_0, the threshold energy of the absorption edge. E_0 was determined as $E_{inf}+\Delta E$, where E_{inf} was the inflection point where the differential coefficient of the spectrum near the absorption edge is maximum and ΔE was allowed to be various fixed values. Reconstruction of the crystalline $LaNi_{5.0}$ spectra can only be achieved using +4.5 eV as ΔE at Ni K-edge and +4.0 eV at La L-edge. Subsequently, $E_0(=E_{inf}+\Delta E)$ was determined with these ΔE values for the amorphous and 80% crystallinity films. Fourier transforms are taken over the range of 3.3—14.0 $Å^{-1}$ and 4.0—9.2 $Å^{-1}$ for the Ni and La edges respectively to obtain the

radial structure function (RSF). In order to obtain the bond distance and the coordination number, the main peaks (Ni; 1.6—2.7 Å, La; 2.4—3.4 Å) were Fourier filtered into the k space, where the inverse Fourier transform was analyzed by the single scattering formula of Stern et al.[11—13] The resulting filtered EXAFS was fitted to the formula of Stern et al., with three variables, namely, B ($=N\times S$; N, true coordination number, S, damping factor which was evaluated from the coordination number of the Ni foil.[14]), apparent coordination number, L, interatomic distance, and σ^2, Debye-Waller factor by means of the nonlinear least square curve-fitting method.[15] Theoretical phase shifts and backscattering amplitudes of Teo and Lee are used in the curve fitting analyses.[16,17] As obtained in general EXAFS measurement,[19,20] the errors in the parameters of B and L were determined as the ranges within which the R value changes by a factor of 2 from the minimum value, with the other parameters held fixed, where R is a reliability factor.

Results and Discussion

Figure 1 illustrates XANES spectra on the Ni K-edge

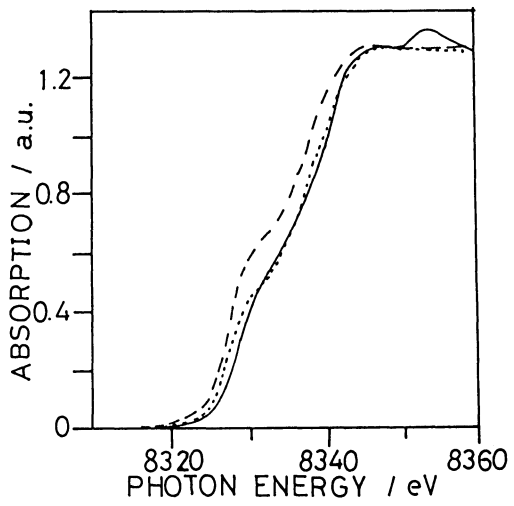

Fig. 1. Ni K-edge XANES spectra for $LaNi_{5.0}$.
——: Ni foil,
– – –: $LaNi_{5.0}$ crystalline bulk,
.....: $LaNi_{5.0}$ amorphous sputtered film.

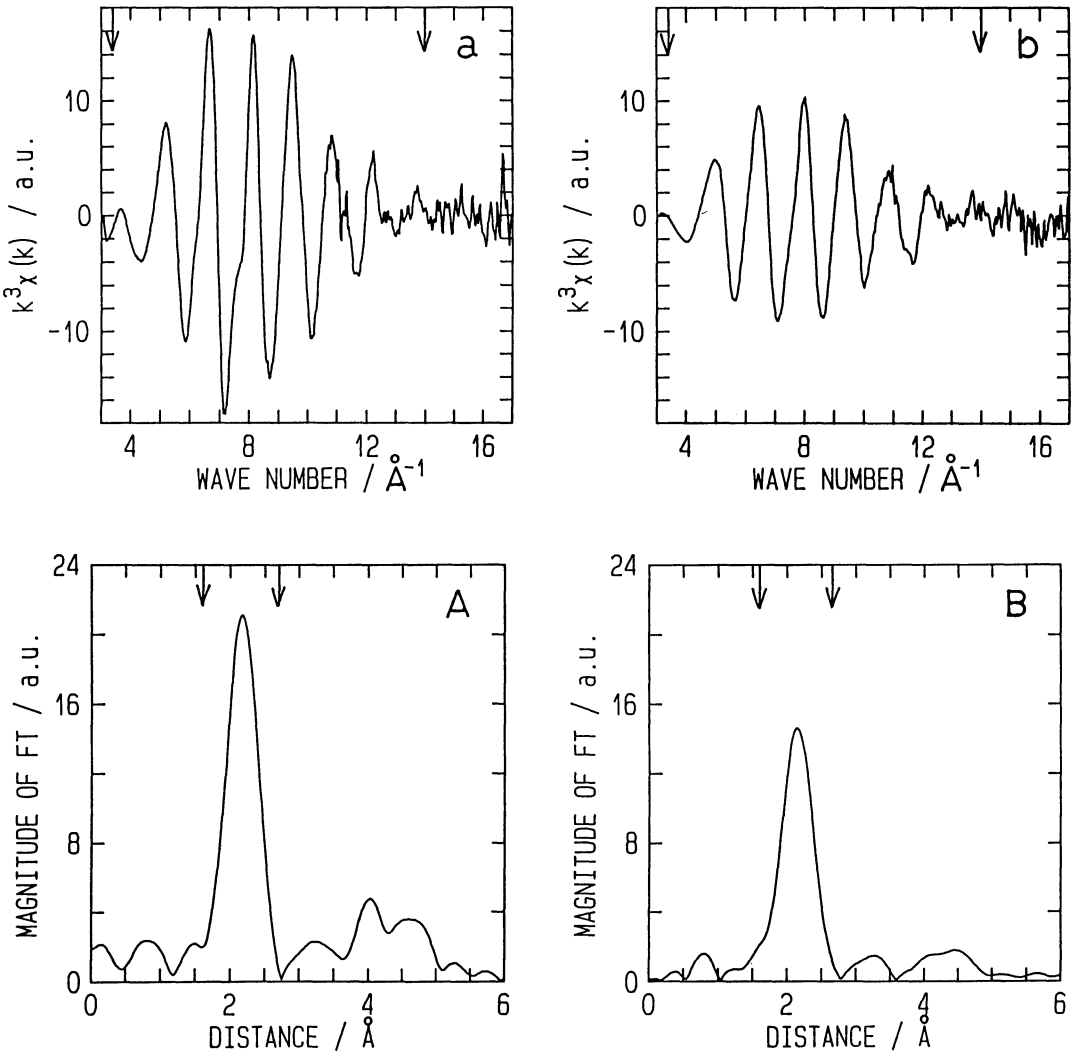

Fig. 2. Ni K-edge k^3-weighted EXAFS spectra (a—b) and magnitudes of their Fourier transforms (A—B), in the 80% crystallinity(a,A) and the amorphous sputtered(b,B) $LaNi_{5.0}$ films. (Arrows (↓) illustrated in the figures indicate the range for Fourier transforms or back Fourier transforms.)

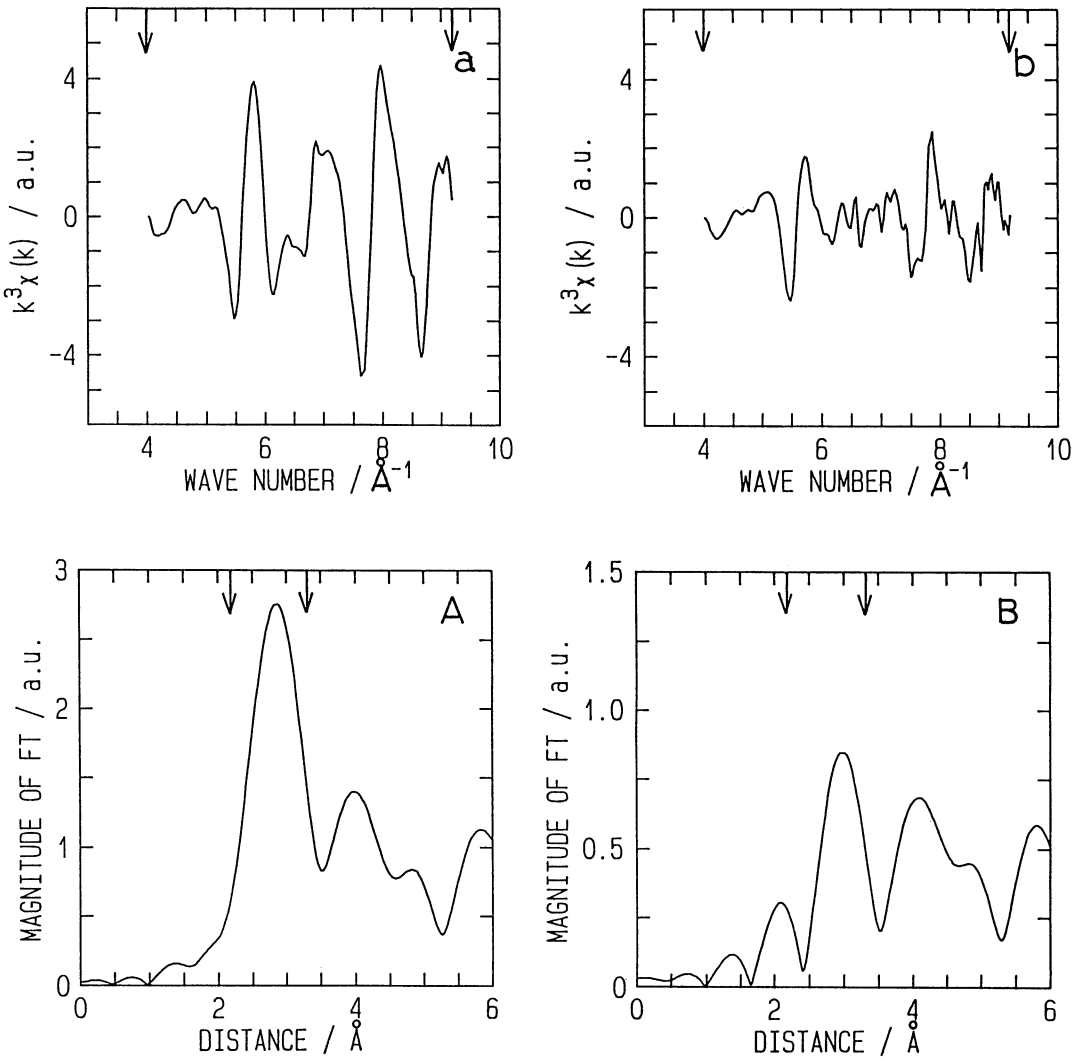

Fig. 3. La L_{III}-edge k^3-weighted EXAFS spectra (a—b) and magnitudes of their Fourier transforms (A—B), in the 80% crystallinity(a,A) and the amorphous sputtered(b,B) $LaNi_{5.0}$ films.

for the Ni foil, the $LaNi_{5.0}$ crystalline bulk and the $LaNi_{5.0}$ amorphous sputtered film. The absorption edge for the $LaNi_5$ crystalline bulk shifted about 1.5 eV to the lower energy side compared with that for the Ni foil due to the narrowing of the Ni 3d-band caused by the charge transfer from the 5d-band of La, which has smaller electronegativity than Ni, to the Ni 3d-band. As for the $LaNi_{5.0}$ amorphous film, the energy position of absorption edge was higher than that for the crystalline bulk. However, no difference of the energy position of absorption edge was observed between the amorphous $LaNi_{5.0}$ film and the Ni foil. This is because the degree of energy transfer from La to Ni for the amorphous film is lower than that for the crystalline bulk.

Figures 2 and 3 show the k^3-weighted EXAFS spectra at the Ni K- and La L_{III}-edges in the sputtered amorphous $LaNi_{5.0}$ films and the 80% crystallinity film. The amplitude of the EXAFS oscillations for the amorphous film was smaller than that for the crystalline film with a crystallinity of 80%. The damping of EXAFS oscillation for the amorphous film seems not to be caused by the decrease in the coordination number, but by the larger static disorder which increases the Debye–Waller factor.

The magnitudes of the Fourier transforms obtained by a Fourier analysis of the EXAFS data in these films are also shown in Figs. 2 and 3. A large peak appeared in these samples on the Ni edge at about 2 Å corresponding to mainly the Ni–Ni and partially Ni–La distance, while on the La edge at about 3 Å corresponding to the La–Ni distance. The profiles of transforms in the sputtered amorphous films show resemblance to that in the 80% crystallinity film, so that it was suggested that the local structures around central Ni and La atoms for the amorphous $LaNi_5$ were similar to those for the crystalline one. The weak intensity of the main peak for the amorphous films was observed on both two edges due to the larger static disorder.

The results of the curve fitting analysis on the Ni edge are presented in Table 1. As for the shortest Ni–

Table 1. Structural Parameters at the Ni K-Edge for $LaNi_{5.0}$[a]

Central atom	Crystalline bulk					80% crystallinity sputtered film				Amorphous sputtered film			
	XRD[b]		EXAFS										
	N	L(Å)	L(Å)	σ^2(Å^2×10^{-3})	R	N	L(Å)	σ^2(Å^2×10^{-3})	R	N	L(Å)	σ^2	R
Ni	4.8Ni	2.461	2.45±0.01	5.2		5.0Ni±0.6	2.46±0.01	5.2		4.6Ni±0.5	2.46±0.01	6.8	
	4 Ni	2.507	2.51±0.01	6.0	3.1×10^{-3}	4.5Ni±1.1	2.56±0.01	8.7	6.2×10^{-3}	3.5Ni±0.9	2.57±0.02	13.2	4.8×10^{-3}
	3 La	2.894	2.89±0.06	8.5		1.4La±1.2	2.90±0.06	8.8		1.7La±1.4	2.92±0.08	14.6	

a) L; interatomic distance, N; real coordination number, σ; Debye–Waller factor, $R=(\{\sum_k[\chi_{obs}(k)-\chi_{calc}(k)]^2\}/[\sum_k\chi_{obs}(k)]^2)^{1/2}$. b) Data from Ref. 18.

Table 2. Structural Parameters at the La L_{III}-Edge for $LaNi_{5.0}$[a]

Central atom	Crystalline bulk					80% crystallinity sputtered film				Amorphous sputtered film			
	XRD[b]		EXAFS										
	N	L(Å)	L(Å)	σ^2(Å^2×10^{-2})	R	B	L(Å)	σ^2(Å^2×10^{-2})	R	B	L(Å)	σ^2	R
La	6 Ni	2.894	2.91±0.03	2.1		1.7±0.1Ni	2.96±0.02	2.0		1.3±0.1Ni	3.01±0.01	2.1	
	12Ni	3.202	3.28±0.01	1.1	1.1×10^{-3}	3.8±0.1Ni	3.28±0.01	1.4	9.8×10^{-4}	2.8±0.2Ni	3.27±0.01	2.1	6.6×10^{-3}

a) L; interatomic distance, B; apparent coordination number, $B=S\times N$, S; damping factor, N; real coordination number, σ; Debye–Waller factor, $R=(\{\sum_k[\chi_{obs}(k)-\chi_{calc}(k)]^2\}/[\sum_k\chi_{obs}(k)]^2)^{1/2}$. b) Data from Ref. 18.

Ni(Ni_I–Ni_{II}) pairs with an interatomic distance of 2.461 Å, the coordination number around Ni_I atoms (CN: 6) is different from that around Ni_{II} atoms (CN: 4), since there are two kinds of Ni atoms (Ni_I and Ni_{II}) having the different symmetry in $LaNi_5$. Therefore, the coordination number for the pairs was estimated with considering the proportion of the number of each Ni atoms in a unit cell. The calculation was performed with the following equation, $(6\times2+4\times3)/5=4.8$.

A fit of the oscillations above the Ni edge was attempted for the crystalline $LaNi_5$ bulk with one shell of Ni atoms. The resulting interatomic distance of the Ni–Ni pair, 2.475 Å, was intermediate between the shortest distance, 2.461 Å, and the second shortest distance, 2.507 Å, which are obtained from XRD analyses,[18] so that it was suggested that the large peak appeared at about 2 Å in the RSF consisted of more than two subshells. When the curve fitting was performed with two subshells of Ni atoms at two different distances from the central atom, the distances of the two Ni–Ni pairs were 2.461 and 2.501 Å respectively. Although these distances were fairly fitted with those estimated from the XRD analyses, the reliability (R) and Debye–Waller (σ^2) factors were still large. Therefore, the interatomic distances were determined by adding one subshell of La atoms at a larger distance (2.89 Å) to the two subshells of Ni atoms. The combination of these three subshells could simulate the spectrum, since both R and σ^2 factors were smaller than the result obtained from the curve fitting with two Ni subshells. For the crystalline bulk, the coordination number obtained with EXAFS is not listed in the table because the XAS was not satisfactory.

The structural parameters of the amorphous film were similar to those of the crystalline bulk though there is the slight difference in the interatomic distance. This indicates that the sites accommodated with hydrogen atoms in the amorphous film were analogous to those in the crystalline bulk. The distances of second Ni–Ni pairs were found to increase about 0.06 Å for the amorphous films in comparison with those for the crystalline bulk. The parameters of interatomic distances for the amorphous sputtered film were slightly different from those for the crystalline film which has a crystallinity of 80%.

The structural parameters for the La edge are summarized in Table 2. The coordination number listed in the table is a tentative value because no adequate result for the $LaNi_{5.0}$ powder as a reference material was obtained from the EXAFS analysis due to inhomogeneities of the particle size in the sample layer.

Lanthanum atoms in the crystalline bulk are known to be coordinated by two kinds of nickel atoms (La–Ni_I; ca. 2.9 Å, La–Ni_{II}; ca. 3.2 Å). For the curve fitting analyses on La L_{III}-edges, the inverse Fourier transform of calculated EXAFS with these two subshells of La–Ni pairs fairly agree with that of experimental EXAFS. The ca. 0.1 Å lengthening of La–Ni_I pairs were found for

the amorphous films in comparison with those for the crystalline bulk. On the Ni K-edge, however, it was not possible to evaluate the differences of Ni_I–La distances between the amorphous film and the crystalline bulk because of large uncertainties in these parameters due to small contribution of the Ni_I–La third subshell to the first nearest neighbor shell consisted of Ni_I–Ni_{II}, Ni_{II}–Ni_{II}, and Ni_I–La subshells.

$LaNi_5$ crystallizes with a hexagonal $CaCu_5$-type structure ($P6/mmm$ space group). The structure consists of two alternating types of plane, the basal plane being consisted of lanthanum and nickel atoms (Ni_I), while the $z=1/2$ plane being consisted of only nickel atoms (Ni_{II}). There are at least three models used to describe the structure of $LaNi_5$ hydride.[21–23] We employed to the model reported by Lartigue et al.,[21], because the refinement of neutron powder diffraction data for their analyses gave better reliability factors. According to the model ($P6_3mc$ space group), as shown in Fig. 4, there are three types of sites (D1, D3, and D5 sites) occupied with hydrogen or deuterium atoms for the crystalline bulk. On the D1 site (2b), hydrogen atoms are found nearly at the center of the Ni_4 tetrahedra ($3Ni_I+1Ni_{II}$). On 6c sites, D3 and D5 atoms are displaced by about 0.4 Å from the center of both the tetrahedra[two lanthanum and two nickel atoms (Ni_{II})], and octahedra[two lanthanum and four nickel atoms ($2Ni_I+2Ni_{II}$)]. On the local structures obtained from the EXAFS analyses, the La and Ni environments do not vary much from the crystalline bulk to the amorphous film, as was suggested by the fact that the Fourier transforms do not change much on the La and Ni edges. Moreover, the Ni–Ni and La–Ni distributions in the amorphous film still have some resemblance to the crystalline bulk, so that the three types of hydrogen sites (D1, D3, and D5) appear to exist in the amorphous film as well as the crystalline bulk. As mentioned above, however, the Ni_{II}–Ni_{II} and La–Ni_I distances were lengthened compared with those for the crystalline bulk, consequently, a part of these three hydrogen sites existed in the crystalline bulk become somewhat distorted. Since the hydrogen atoms appears to be difficult to be stably located in the sites distorted, the amount of hydrogen taken up by the amorphous $LaNi_{5.0}$ is smaller than that by the crystalline one.

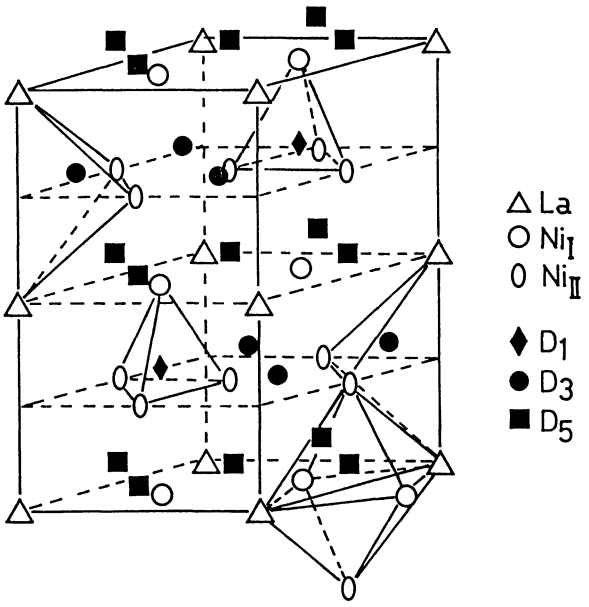

Fig. 4. Structure of the hypothetical fully ordered $LaNi_5D_7$ phase involving three types of sites occupied with hydrogen.

Conclusion

The local structures around La and Ni atoms in amorphous $LaNi_5$ films have been clarified with EXAFS. The distortion of three kinds of sites in which hydrogen atoms are considered to occupy was observed in the amorphous films due to the lengthening of interatomic distances in the Ni–Ni and La–Ni pairs. If the hydrogen atoms become difficult to be stably located in the sites, the hydrogen content in the amorphous $LaNi_{5.0}$ would be smaller than that in the crystalline one.

We thank Dr. M. Nomura and the staff of the Photon Factory at KEK for their helpful advice and technical assistance in the EXAFS measurement. This work was partially supported by a Grant in Aid for Developmental Scientific Research Nos. 63850167 and 01470074 for G. Adachi, and No. 63790311 for H. Sakaguchi, from the Ministry of Education, Science and Culture.

References

1) G. Adachi, H. Nagai, and J. Shiokawa, *J. Less-Common Met.*, **97**, L9 (1984).
2) H. Sakaguchi, G. Adachi, and J. Shiokawa, *Bull. Chem. Soc. Jpn.*, **61**, 521 (1988).
3) H. Sakaguchi, Y. Yagi, J. Shiokawa, and G. Adachi, *J. Less-Common Met.*, **149**, 185 (1989).
4) G. Adachi, H. Sakaguchi, K. Niki, H. Nagai, and J. Shiokawa, *Bull. Chem. Soc. Jpn.*, **58**, 885 (1985).
5) H. Sakaguchi, N. Taniguchi, H. Nagai, K. Niki, G. Adachi, and J. Shiokawa, *J. Phys. Chem.*, **89**, 5550 (1985).
6) H. Sakaguchi, N. Taniguchi, H. Seri, J. Shiokawa, and G. Adachi, *J. Appl. Phys.*, **64**, 888 (1988).
7) H. Sakaguchi, H. Seri, and G. Adachi, *J. Phys. Chem.*, **94**, 5313 (1990).
8) B. J. Jan, H. J. Klabunde, T. Tanaka, H. Kanai, and S. Yoshida, *J. Am. Chem. Soc.*, **110**, 5951 (1988).
9) H. Yamashita, H. Mizutani, T. Tanaka, T. Funabiki, and S. Yoshida, *J. Non-Cryst. Solids*, **95 & 96**, 419 (1987).
10) T. Tanaka, H. Yamashita, R. Tsuchitani, T. Funabiki, and S. Yoshida, *J. Chem. Soc.*, **84**, 2987 (1988).
11) E. A. Stern, *Phys. Rev. B*, **10**, 3027 (1974).
12) C. A. Ashley and S. Doniach, *Phys. Rev. B*, **11**, 1279 (1975).
13) P. A. Lee and J. B. Pendry, *Phys. Rev. B*, **11**, 2795 (1975).
14) A. Taylor, *J. Inst. Met.*, **77**, 585 (1950).
15) K. Levenberg, *Q. Appl. Math.*, **2**, 164 (1944).

16) B. K. Teo, P. A. Lee, A. L. Simons, P. Eisenberger, and B. M. Kincaid, *J. Am. Chem. Soc.,* **99**, 3854 (1977).
17) P. A. Lee, B. K. Teo, and A. L. Simons, *J. Am. Chem. Soc.,* **99**, 3856 (1977).
18) M. Gupta, *J. Less-Common Met.,* **130**, 219 (1987).
19) T. Claeson, J. B. Boyce, P. W. Lowe, and T. H. Gaballe, *Phys. Rev. B,* **29**, 4969 (1984).
20) B. Lengeler and P. Eisenberger, *Phys. Rev. B,* **21**, 4507 (1980).
21) C. Lartigue, A. Le Bail, and A. Percheron-Guegan, *J. Less-Common Met.,* **129**, 65 (1987).
22) H. Hayakawa, K. Nomura, Y. Ishido, Y. Akiba, and S. Shin, *J. Less-Common Met.,* **143**, 315 (1988).
23) P. Thompson, J. J. Reilly, L. M. Hastings, and R. Hempelmann, *J. Phys. F,* **16**, 675 (1986).